Hindawi
Advances in Civil Engineering
Volume 2023, Article ID 9898510, 1 page
https://doi.org/10.1155/2023/9898510

*Retraction*

# Retracted: Energy Evolution Characteristics and Performance Parameter Degradation of Rubber-Mixed Concrete in Sulfate Attack Environment

**Advances in Civil Engineering**

Received 10 October 2023; Accepted 10 October 2023; Published 11 October 2023



This article has been retracted by Hindawi following an investigation undertaken by the publisher [1]. This investigation has uncovered evidence of one or more of the following indicators of systematic manipulation of the publication process:

(1) Discrepancies in scope
(2) Discrepancies in the description of the research reported
(3) Discrepancies between the availability of data and the research described
(4) Inappropriate citations
(5) Incoherent, meaningless and/or irrelevant content included in the article
(6) Peer-review manipulation

The presence of these indicators undermines our confidence in the integrity of the article's content and we cannot, therefore, vouch for its reliability. Please note that this notice is intended solely to alert readers that the content of this article is unreliable. We have not investigated whether authors were aware of or involved in the systematic manipulation of the publication process.

Wiley and Hindawi regrets that the usual quality checks did not identify these issues before publication and have since put additional measures in place to safeguard research integrity.

We wish to credit our own Research Integrity and Research Publishing teams and anonymous and named external researchers and research integrity experts for contributing to this investigation.

The corresponding author, as the representative of all authors, has been given the opportunity to register their agreement or disagreement to this retraction. We have kept a record of any response received.

## References

[1] X. Chen, "Energy Evolution Characteristics and Performance Parameter Degradation of Rubber-Mixed Concrete in Sulfate Attack Environment," *Advances in Civil Engineering*, vol. 2022, Article ID 5692655, 10 pages, 2022.

Hindawi
Advances in Civil Engineering
Volume 2022, Article ID 5692655, 10 pages
https://doi.org/10.1155/2022/5692655



*Research Article*

# Energy Evolution Characteristics and Performance Parameter Degradation of Rubber-Mixed Concrete in Sulfate Attack Environment

**Xiu-ling Chen**

*School of Architectural Engineering, Ma'anshan University, Ma'anshan 243000, China*

Correspondence should be addressed to Xiu-ling Chen; chenxl_1990@126.com

Received 21 December 2021; Revised 12 January 2022; Accepted 13 January 2022; Published 30 January 2022

Academic Editor: Ramadhansyah Putra Jaya



In order to study the sulfate resistance of rubber concrete (RC), the compressive strength test of RC with different contents (0%, 5%, 10%, and 15%) was carried out, and the proportion of RC with standard curing for 28 days was optimized. Sulfate attack test was carried out on the selected RC and compared with normal concrete (NC). The degradation degree was measured from the effective porosity, relative dynamic elastic modulus, $SO_4^{2-}$ concentration, and SEM microstructure observation after different attack times. The energy analysis method is used to study the evolution law of total strain energy, elastic strain energy, and dissipated strain energy of NC and RC in the process of deformation and failure after different attack times, and the influence of sulfate attack on concrete is explored from the perspective of energy. The results show that with the progress of sulfate attack, the effective porosity of NC and RC both decreases first and then increases, and the relative dynamic elastic modulus increases first and then decreases. Rubber is beneficial to improve the sulfate resistance of concrete, delay the attack of $SO_4^{2-}$ on concrete, and improve the ductile deformation of concrete. This study can provide a theoretical reference for the application of RC in practical engineering.

## 1. Introduction

As the most widely used and most basic building material, concrete is increasingly applied into the fields of civil engineering, transportation, water conservancy and hydropower, etc. Its durability has become a key engineering issue and has received widespread attention [1, 2]. Among them, sulfate erosion is one of the important factors. Essentially, sulfate ions react with cement hydrates to produce expansions that result in concrete damage and destruction, which affects the durability of concrete and reduces the strength of concrete. There are high concentrations of sulfate ions in the saline soil environment, and the long-term sulfate erosion of concrete reduces the structural safety of concrete and also shortens the service life [3, 4].

Currently, many scholars have done researches on the reduction of concrete durability caused by sulfate attack. Wang et al. [5] conducted an experimental study on the law and mechanism of concrete durability degradation, whose results showed that the durability damage of sulfate attack on concrete was much greater than compound salt attack. Wu et al. [6] carried out researches on the durability of concrete under sulfate erosion environment based on the theory of damage mechanics and found that with the increase of erosion time, the coexpansion of ettringite and gypsum caused microcracks and the number continued to increase. Wang et al. [7] studied the changing characteristics of concrete pore structure under sulfate attack and analyzed the microstructure and mineralogical composition. Jin et al. [8] conducted an experimental study on the damage process of concrete in a sulfate attack environment, and the results showed that sulfate attack caused the expansion of concrete and formed a large number of cracks, which deteriorated the performance of concrete. Zhao et al. [9] studied the acoustic emission and physical and mechanical properties of concrete under the two sulfate erosion conditions of continuous

soaking and dry-wet cycle. They found that the dry-wet cycle accelerated the deterioration of concrete. The pores inside the concrete increased the strength of the concrete to a certain extent.

In order to improve the resistance of concrete to sulfate corrosion and extend the service life of the building, Sharma and Khan [10] used copper slag to replace parts of the fine aggregate in concrete to study the sulfate corrosion resistance and found that the copper slag replaces 40% of the fine aggregate, which was beneficial to improve the compressive strength of concrete and the resistance to sulfate attack. Wang et al. [11] studied the performance degradation of basalt fiber concrete under sulfate erosion environment and found that basalt fiber had a certain increase in the bearing capacity and deformation capacity of concrete and could delay the increase of concrete porosity. Lv et al. [12] studied the sulfate corrosion resistance and mechanism of silica fume-reinforced cement mortar. Vishwakarma et al. [13] separately incorporated fly ash and nano-$TiO_2$ into concrete to compare and analyze the sulfate erosion resistance and found that the fly ash concrete had better sulfate erosion resistance.

With the rapid development of the global economy, the rapid growth of annual automobile sales has caused a sharp increase in the amount of discarded rubber tires each year. As discarded tires are solid wastes that are not easily degradable, they have caused serious pollution [14, 15]. Studies have shown [16–18]: substituting rubber particles for part of the fine aggregate in concrete can not only solve the environmental pollution caused by discarded tires and save resources, but also make the concrete have good toughness, excellent impermeability, and antipermeability, together with good freezing performance and high ductility. Strukar et al. [19] conducted a uniaxial compression test on RC to explore the influence of rubber content on the mechanical behavior of concrete, conducted a comprehensive study on its stress-strain curve, and found that rubber could enhance the ductility of concrete. Ridgley et al. [20] used acoustic emission technology to study the abrasion resistance of NC and RC, and found that the quality loss and wear depth of RC were significantly lower than that of NC. Zhang et al. [21] studied the effect of rubber on the frost resistance of concrete and found that rubber could effectively reduce the damage of concrete in a freeze-thaw cycle environment and improve its freeze-thaw cycle resistance. Alwesabi et al. [22] found that rubber can enhance the fracture toughness of concrete.

In this paper, rubber is mixed into concrete, and the rubber dosage is optimized to carry out the sulfate corrosion test and use NC as a reference, and reveals the law of rubber to improve the sulfate corrosion resistance of concrete, providing theoretical support for related engineering practice.

## 2. Experiment

*2.1. Raw Materials.* The raw materials are as follows—cement: P·O 42.5 grade ordinary Portland cement; stone: continuous graded crushed stones with particle sizes of 5~15 mm; sand: medium sand with a fineness modulus of 2.55; rubber: particle sizes of 1~3 mm with a density of 1050 kg/m$^3$; sulfate: analytically pure AR-type anhydrous sodium sulfate; water reducing agent: HPWR-type high-performance water reducing agent; and water: tap water.

*2.2. Design of Mix Proportion.* The purpose of the experimental design in this paper is to reveal the degradation law of RC performance under sulfate attack. According to the National Standard of the People's Republic of China GB/T 50082-2009 *Standard for Test Methods of Long-term Performance and Durability of Ordinary Concrete*, the sulfate solution concentration is selected as 5%. Referring to the National Standard of the People's Republic of China JGJ 55-2011 *Specification for Mix Proportion Design of Ordinary Concrete,* the design of the concrete mix proportion was carried out. In this experiment, the rubber contents are 0%, 5%, 10%, and 15% of the sands quality, respectively. The specific mix proportions are listed in Table 1.

According to the relevant provisions of the National Standard of the People's Republic of China GB/T 50081-2019 *Standard for Test Methods of Concrete Physical and Mechanical Properties*, CSS-YAN 3000 press is used for compressive strength test, and the test results are shown in Figure 1. It can be summarized that with the increase of rubber content, the compressive strength of concrete increases first and then decreases. When the rubber content is less than 10%, the strength of rubber concrete is improved, compared with that of NC. But with the further increase of rubber content, the concrete strength begins to decrease. When the rubber content is 10%, the strength growth rate is the largest, and compared with NC, it is increased by 22.20%. It can be seen from Figure 1(b) that the stress-strain curves of NC and RC are similar on the whole. With the increase of rubber content, the stress-strain curve's rising speed is more rapid than that of NC, and the decline rate of the curve after the peak stress decreases, which shows that the addition of rubber into concrete is conducive to improving the ductility and deformation of concrete. This is mainly because rubber improves the gradation of sands, enhances the adhesion between cement and sands, and improves the workability of concrete. However, too much rubber will reduce the cement hydration reaction of concrete, and the amount of sands will be greatly reduced, resulting in the decrease of strength, which is consistent with relevant studies [23].

*2.3. Sulfate Erosion Experiment Schemes.* In the sulfate erosion test, the RC content is 10%, that is, the mix proportion of $RC_2$ group. The size of the concrete specimen is 100 mm × 100 mm × 100 mm, which has been cured for 28 days at a relative humidity of 95% or so under a temperature zone from 18°C to 22°C. With the concentration of the sulfate solution being 5%, the experiment is carried out to test the performance degradation process of RC in a sulfate erosion environment and compare it with NC by following alternating dry and wet methods. The specific operation process is in accordance with the National Standard of the People's Republic of China GB/T 50082-2009 *Standard for Test Methods of Long-term Performance and Durability of*

Table 1: Mix proportion (kg/m$^3$).

| Specimen | Cement | Stone | Sand | Rubber | Water | Water reducing agent |
|---|---|---|---|---|---|---|
| NC | 425 | 1185 | 650 | 0 | 195 | 5.25 |
| $RC_1$ | 425 | 1185 | 617.5 | 32.5 | 195 | 5.25 |
| $RC_2$ | 425 | 1185 | 585 | 65 | 195 | 5.25 |
| $RC_3$ | 425 | 1185 | 552.5 | 97.5 | 195 | 5.25 |

*Ordinary Concrete*. The drying temperature was 85°C, and the alternating time was 72 hours. The dry and wet ratio was 3 : 1, and the number of dry and wet alternates was set to 15 times, 30 times, 45 times, 60 times, 75 times, and 90 times, respectively. In view of the fact that $SO_4^{2-}$ will react with the calcium silicate hydrate in the concrete during the erosion process, the $SO_4^{2-}$ of the erosion solution will decrease. Therefore, the sulfate solution was changed every 30 days.

After reaching the predetermined number of dry and wet alternations, the saturated mass and dry mass of the test piece were weighed to calculate the effective porosity of the test piece. The calculation formula shall be carried out according to formula (1); the HC-U81 nonmetal ultrasonic detector was applied to detect the ultrasonic sound of the test piece at each predetermined number of dry and wet alternations. When calculating the relative dynamic elastic modulus of the test piece, Equation (2) was carried out.

$$w = \frac{m_s - m_d}{m_d}, \tag{1}$$

where $w$ is the effective porosity; $m_s$ is the saturated mass (kg); and $m_d$ is the dried mass (kg).

$$E = \left(\frac{T_0}{T_t}\right)^2, \tag{2}$$

where $E$ is the relative dynamic modulus of elasticity; $T_0$ is the uncorroded ultrasonic duration (s); and $T_t$ is the ultrasonic duration (s) when eroded $t$ times.

*2.4. Principle of Energy Conversion.* Energy conversion is the essential feature of the physical process of matter. The deformation and failure process of concrete under load is essentially the process of energy evolution inside concrete and energy exchange with the outside world. With the continuous action of the load, the energy input from the outside is gradually transformed into elastic strain energy, dissipation energy, electromagnetic energy, radiation energy, and so on of concrete. Since the proportion of electromagnetic energy and radiant energy is very small under static action, the main energy conversion relationship of concrete under load is seen in

$$U = U_e + U_d, \tag{3}$$

where $U$ is the total strain energy per unit volume; $U_e$ is the elastic strain energy per unit volume; and $U_d$ is the dissipated strain energy per unit volume.

According to the stress-strain relationship, the total strain energy and elastic strain energy input by external force of concrete specimen per unit volume are seen in.

$$U = \int \sigma d\varepsilon, \tag{4}$$

$$U_e = \frac{\sigma^2}{2E}, \tag{5}$$

where $\sigma$ is the axial stress; $\varepsilon$ is the axial strain; and $E$ is the initial elastic modulus.

Therefore, the dissipated strain energy per unit volume is

$$U_d = U - U_e. \tag{6}$$

It should be pointed out that the initial defects inside the specimen have been closed to a certain extent because the concrete specimen has been repeated preloading and unloading before formal loading. Therefore, $E$ is taken as the slope of the straight line between 10% and 30 of the peak stress at the initial stage of the stress-strain curve of the specimen.

## 3. Experimental Results and Analysis

*3.1. Stress-Strain Curve.* The stress-strain curves of NC and RC in the sulfate attack environment are shown in Figure 2. It can be seen that with the progress of sulfate erosion, the stress-strain curves of NC and RC have undergone significant changes, but on the whole, the changes of NC are more obvious; as the dry-wet cycles' times increase, the stress-strain curve moves toward the right direction that deviates from the $Y$-axis. The stress and strain peaks of NC and RC increase first and then decrease as a whole, and the stress peak of RC increases rapidly in the early stage of erosion and then the speed being slower. The deformation of RC in the linear elastic stage is lighter. After 30 times' dry-wet cycles, the peak stress of NC came to the biggest. Compared with the uneroded specimen, the peak stress increases by 7.24%. After 60 times' dry-wet cycles, the peak stress of RC is the largest. Compared with the uneroded specimen, the peak stress increases by 11.66%. After 90 times' dry-wet cycles, the stress and strain peaks of NC and RC decrease at the same time in different levels. Compared with the uneroded specimen, the peak stress of NC and RC decreases by 28.04% and 8.6%, respectively.

The change rules of compressive strength with sulfate erosion are shown in Figure 3. Based on Figure 3, it can be seen that at the same sulfate attack time, the compressive strength of RC is greater than that of NC. As the erosion progresses, the compressive strength of RC is comparable to that of the predetermined number of dry-wet cycles. Compared with NC, it increased by 22.20%, 21.88%, 22.66%, 38.84%, 52.48%, 48.50%, and 55.19%, respectively. It can be seen that in the environment of sulfate erosion, rubber is beneficial to increase the compressive strength of concrete, improve the deterioration performance of concrete, and enhance the sulfate erosion resistance. The longer the erosion time is, the more obvious the effects are.

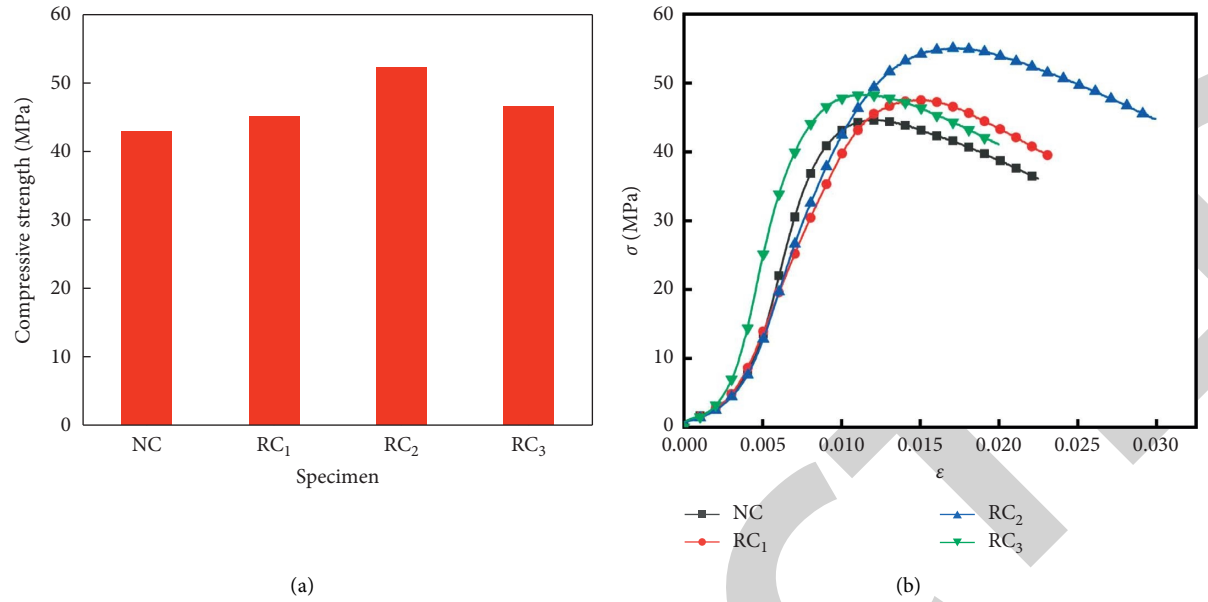


Figure 1: Test results. (a) Compressive strength. (b) Stress-strain curves.

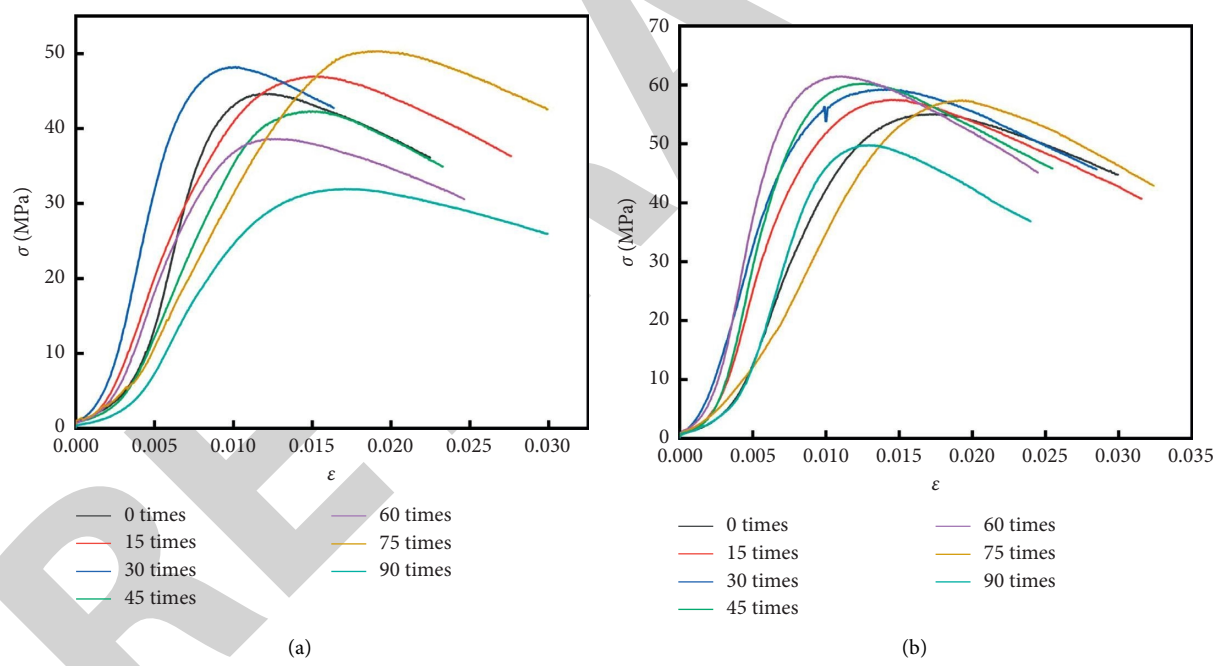


Figure 2: Stress-strain curve. (a) NC. (b) RC.

If it is assumed that the change in compressive strength with sulfate erosion is continuous, the following formula, as shown in equation (7), could be set up under the guidance of the least square method [24].

$$f = a + bt + ct^2, \tag{7}$$

where $f$ is the compressive strength; $a$, $b$, and $c$ are fitting parameters; and $t$ is the number of dry-wet cycles. The fitting result is shown in Figure 4. The strength damage evolution equation is shown as follows:

$$\begin{aligned} f_{cn} &= 43.54 + 0.08296t - 0.00261t^2\left(R^2 = 0.92\right), \\ f_{cr} &= 51.38 + 0.31714t - 0.00383t^2\left(R^2 = 0.86\right), \end{aligned} \tag{8}$$

where $f_{cn}$ and $f_{cr}$, respectively, represent the compressive strength of NC and the compressive strength of RC.

*3.2. Energy Evolution.* Figure 5 shows the evolution of the total strain energy of NC and RC in a sulfate attack environment. Figure 6 shows the evolution of the dissipated

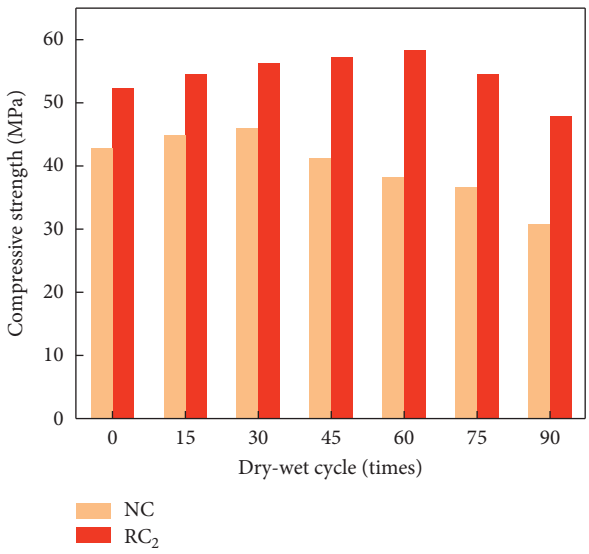


Figure 3: Compressive strength.

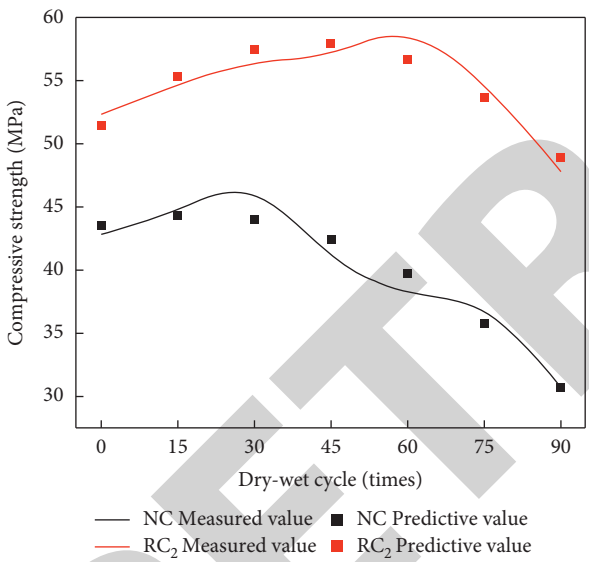


Figure 4: Compressive strength damage evolution fitting curve.

strain energy of NC and RC in the sulfate erosion environment. It can be seen from Figures 5 and 6 that the total strain energy and dissipation strain energy of NC and RC increase firstly and then decrease. Under the same number of dry-wet cycles, the total strain energy and dissipated strain energy of RC are greater than that of NC. In the early stage of erosion, the growth rate of total strain energy and dissipated strain energy of RC is greater than that of NC. In the later stage of erosion, the rate of decrease of total strain energy and dissipated strain energy of RC is lower than that of NC. With the increase in deformation, the incorporation of rubber into concrete can obviously speed up the rate of total strain energy and dissipated strain energy. When the specimen finally fails, the total strain energy of RC is increased by 41.21%, 52.36%, 60.64%, 68.39%, 69.80%, 22.85%, and 17.84%, respectively, compared with NC under the same number of dry-wet cycles. Bulk strain energy is increased by 37.98%, 43.72%, 49.79%, 54.28%, 60.34%, 33.39%, and 22.15%, respectively.

Figure 7 shows the evolution law of elastic strain energy of NC and RC in a sulfate attack environment. It can be seen that the change law of rubber to concrete elastic strain energy is similar to the total strain energy and dissipation energy. At the same predetermined number of dry-wet cycles, the elastic strain energy of NC decreases faster than RC as a whole when reaching its peak value, showing more obvious brittle failure, while RC shows more obvious ductile failure. This is mainly because rubber improves the gradation of sands, which can inhibit coupling, crack penetration speed and propagation speed, and improve the toughness and failure characteristics of concrete [25].

*3.3. Deterioration of Performance Parameters.* In order to deeply explore the internal damage of NC and RC by sulfate, the effective porosity and relative dynamic elastic modulus of concrete are used as performance parameters. The effective porosity and relative dynamic elastic modulus changes are shown in Figures 8 and 9.

It can be seen from Figure 8 that both NC and RC show a trend of first decreasing and then increasing with the progress of sulfate erosion. This is related to the above-mentioned compressive strength test; that is, as the effective porosity of concrete decreases, the interior of the concrete is dense. The higher the degree, the higher the intensity is. For NC, the effective porosity is the lowest when the dry-wet cycles being 45 times, and the lowest effective porosity of RC appears when the dry-wet cycles being 60 times; the effective porosity of NC is basically lower than that of RC, which shows that in sulfuric acid in a salt-eroded environment, the internal porosity of NC increases, while RC optimizes the particle gradation of cementing materials due to the rubber, which makes the concrete cement hydration reaction more sufficient and the density is improved.

It can be seen from Figure 9 that the relative dynamic elastic modulus of NC and RC increases first and then decreases with the progress of sulfate erosion. The peak value of the relative dynamic elastic modulus of NC appears at 45 times of dry-wet cycle, and then the relative dynamics elastic modulus drops rapidly. When the dry-wet cycles mounting to 90 times, the relative dynamic elastic modulus is lower than 0.75, which indicates that NC has reached the damage limit at this time; the relative dynamic elastic modulus of RC changes more slowly than NC. The peak value of the relative dynamic elastic modulus appeared at 60 times of dry-wet cycle and then began to decrease. When dry-wet cycles mounting to 90 times, the relative dynamic elastic modulus of RC was higher than 0.75, which did not reach the damage limit.

*3.4. $SO_4^{2-}$ Concentration Distribution Law.* Figure 10 shows the change of $SO_4^{2-}$ content in NC and RC after 45 times' dry-wet cycles. It can be seen that the $SO_4^{2-}$ concentration of each group of specimens shows a downward trend, and as the depth deepens, the decreasing rate becomes faster and

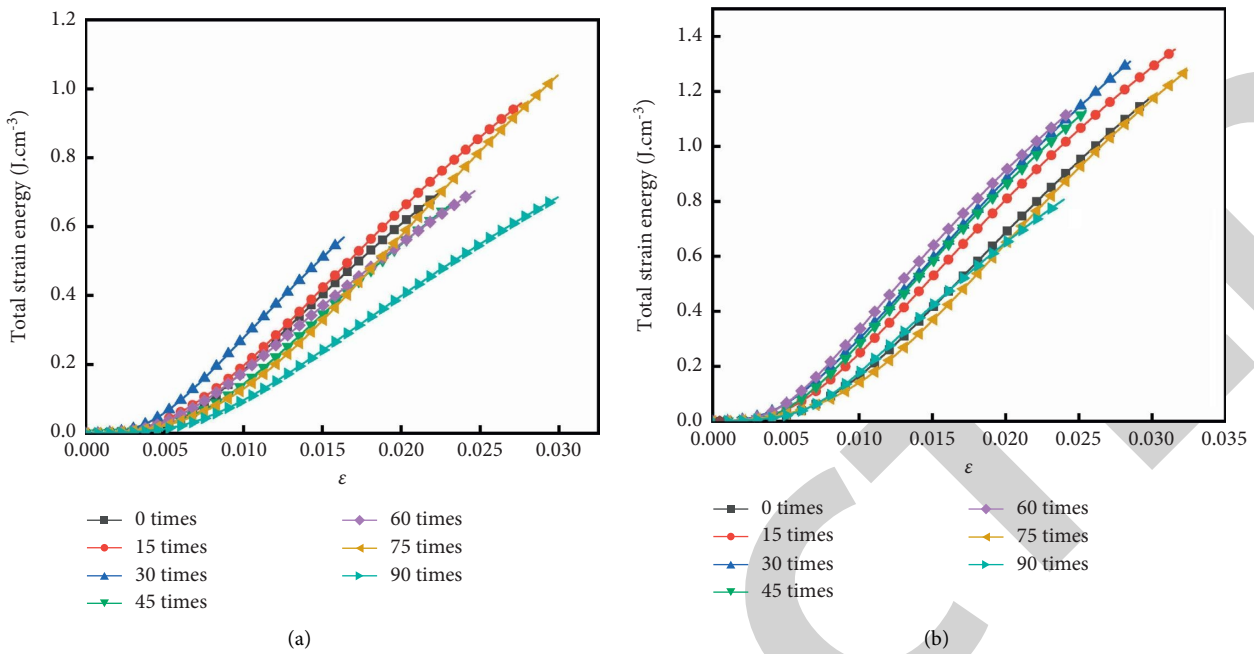


Figure 5: Total strain energy. (a) NC. (b) RC.

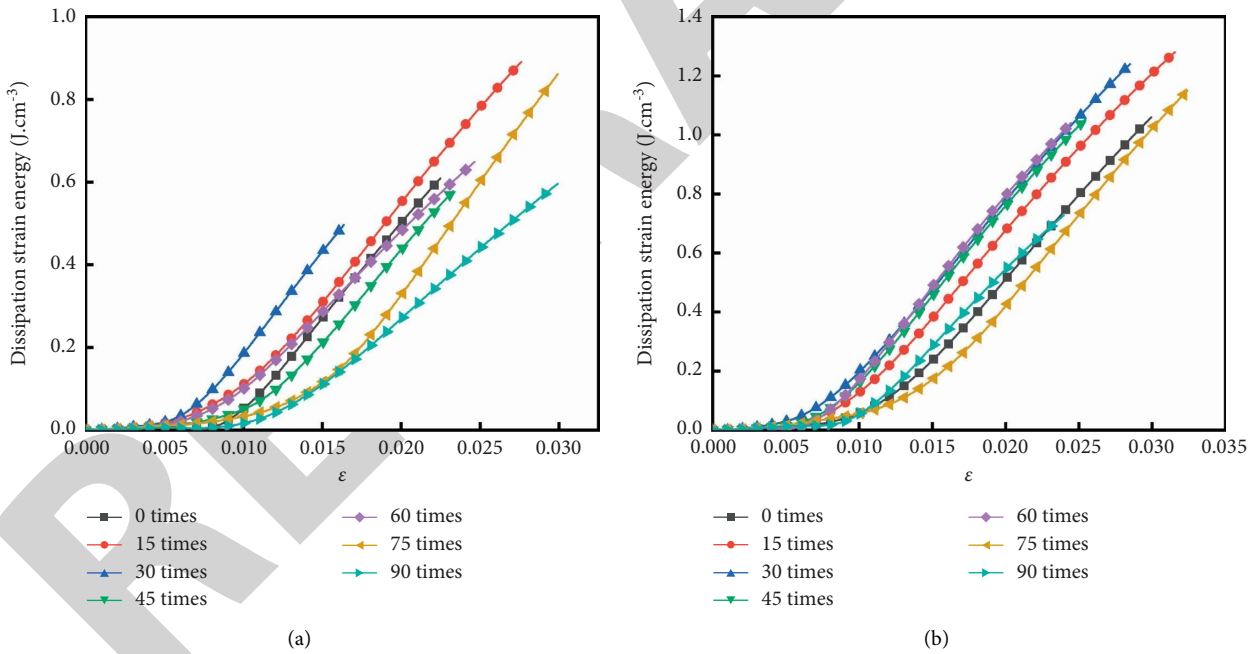


Figure 6: Dissipation strain energy. (a) NC. (b) RC.

faster. The $SO_4^{2-}$ content gradually decreases with the increase of the penetration depth; because the surface concrete is in the influence depth range, a large amount of solution is sucked inside, so that $SO_4^{2-}$ has a relatively high concentration on the surface of the concrete; as the depth increases, the migration rate of $SO_4^{2-}$ decreases, and the concentration decreases accordingly.

Figure 11 shows the change of $SO_4^{2-}$ content in NC and RC after 90 times' dry-wet cycles. It can be seen that the $SO_4^{2-}$ concentration of each group of test pieces still shows a downward trend. The decrease is slower in the early stage and faster in the later stage. After 90 times' dry-wet cycles, the $SO_4^{2-}$ concentration of each group of test pieces is compared with that of dry-wet cycles. It was higher at 45 times, and the $SO_4^{2-}$ mass fraction from the outer layer to the inner layer also gradually decreased.

According to Figures 10 and 11, it can be seen that the incorporation of rubber into concrete significantly reduces

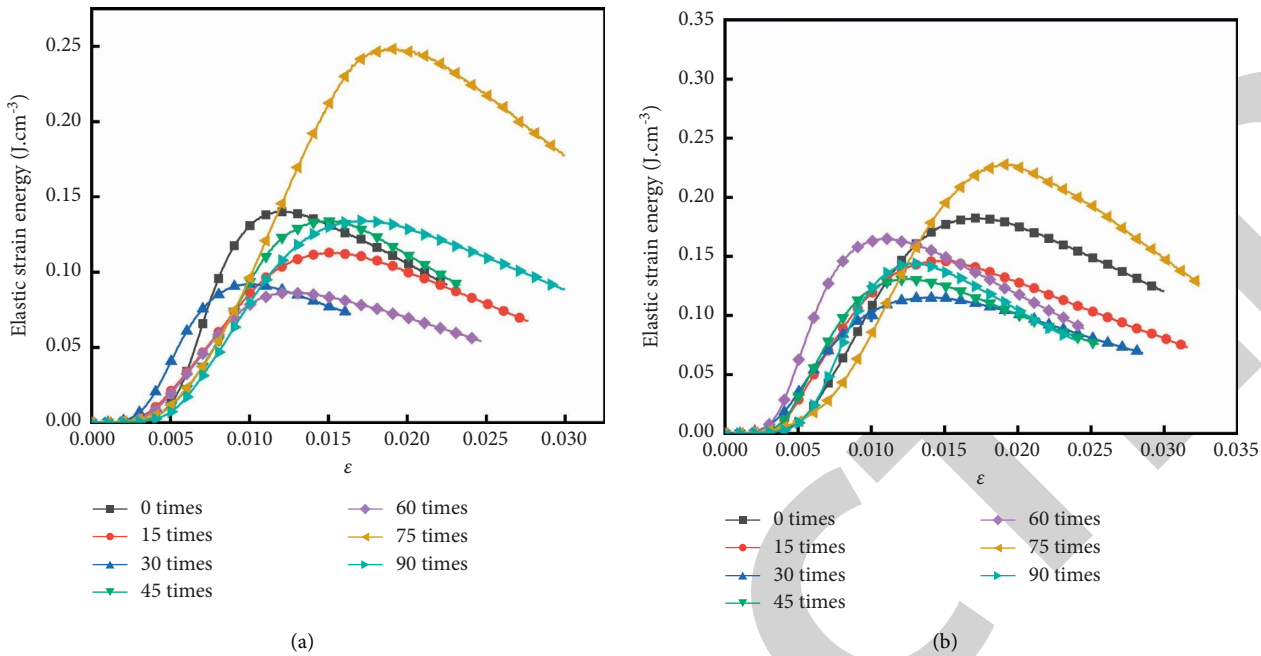


Figure 7: Elastic strain energy. (a) NC. (b) RC.

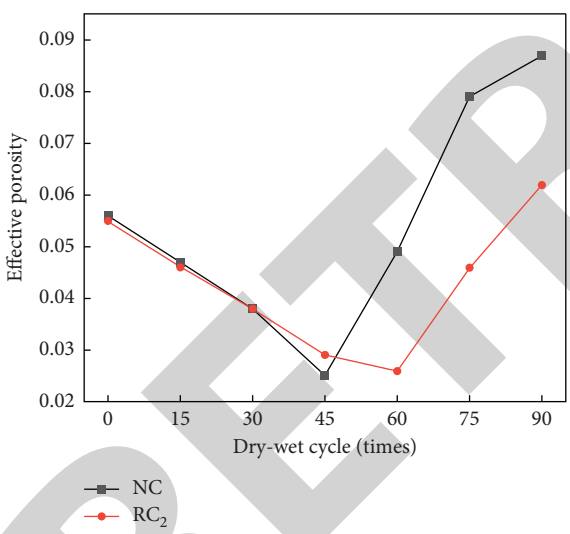


Figure 8: Effective porosity.

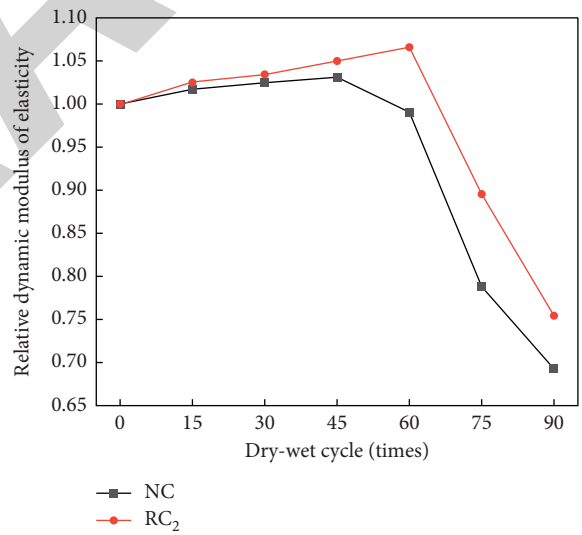


Figure 9: Relative dynamic modulus of elasticity.

the $SO_4^{2-}$ concentration at different depths in the concrete, and the $SO_4^{2-}$ corrosion resistance is in the order of RC group > NC group, which shows that rubber can improve the concrete's $SO_4^{2-}$ corrosion resistance, to reduce the invasion of $SO_4^{2-}$.

## 4. SEM Microanalysis

The deterioration process of concrete in sulfate attack environment can be divided into two stages. In the first stage, due to the difference of $SO_4^{2-}$ concentration between the inside and outside of the concrete sample in the attack solution, the $SO_4^{2-}$ in the solution is continuously transferred to the inside of the concrete, and a series of chemical reactions occur with the $Ca(OH)_2$ and C-S-H gel inside the concrete to form ettringite and gypsum, which fills the pores inside the concrete and effectively reduces the effective porosity of the concrete. In the second stage, as the corrosion progresses, ettringite and gypsum continue to accumulate and fill the internal pores of the concrete to produce expansion force. The expansion force is greater than the tensile strength of the concrete to produce cracks. The gradual increase of cracks accelerates the $SO_4^{2-}$ intrusion to generate more ettringite and gypsum, which eventually leads to structural expansion failure and sharp decline in mechanical properties [9, 26].

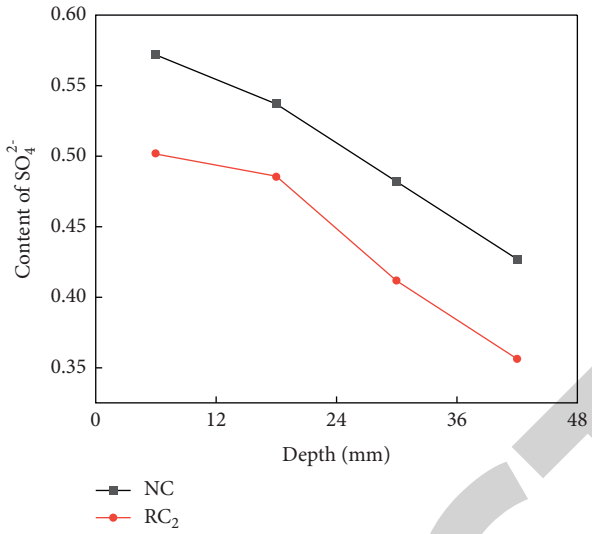


Figure 10: $SO_4^{2-}$ content of NC and RC when dry-wet cycle being 45 times.

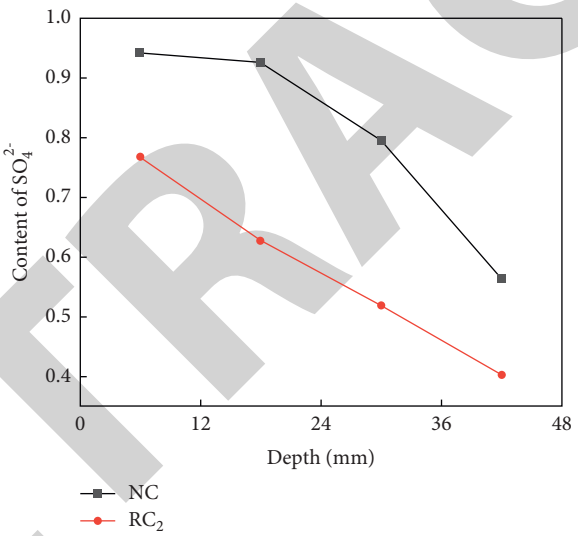


Figure 11: $SO_4^{2-}$ content of NC and RC when dry-wet cycle being 90 times.

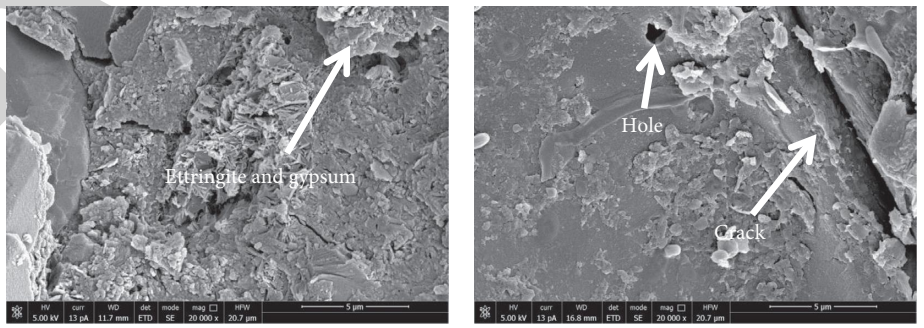


(a) (b)

Figure 12: The microstructure of ordinary concrete under sulfate erosion environment. (a) Dry-wet cycle 45 times. (b) Dry-wet cycle 90 times.

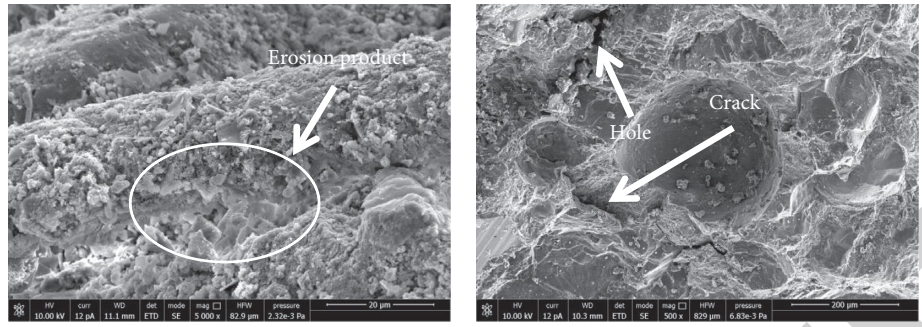


(a) (b)

Figure 13: The microstructure of rubber concrete under sulfate erosion environment. (a) Dry-wet cycle 45 times. (b) Dry-wet cycle 90 times.

The SEM microstructures of ordinary concrete and rubber concrete under sulfate attack environment are shown in Figures 12 and 13, respectively. As the corrosion progresses, there are obvious pores on the surface of ordinary concrete and rubber concrete. In contrast, the pore structure of ordinary concrete is looser. Both types of concrete have a large amount of corrosion products attached inside, indicating that $SO_4^{2-}$ is transferred into the concrete for chemical reaction to produce gypsum. This chemical reaction rapidly consumed the hydroxide radicals inside the concrete and decomposed the C-S-H gel. Hence, the concrete pore increased and gradually developed into cracks, and reduced the concrete density and structural stability. Comparing Figures 12 and 13, it can be found that compared with rubber concrete, ordinary concrete higher content of adhesive mortar, weaker bonding at the interface, large internal holes, and wide cracks, which accelerates the transmission of $SO_4^{2-}$ in the concrete, resulting in the interior structure of ordinary concrete is more loose. By contrast, due to the workability of rubber particles, the particle gradation of aggregate is optimized and the structure is more dense. Therefore, the sulfate resistance of rubber concrete is improved compared with ordinary concrete.

## 5. Conclusion

(1) Mixing a proper amount of rubber particles into concrete can effectively improve the compressive strength of concrete, and the rubber replaces the 10% mass of fine aggregate that is the optimal, which is 22.20% higher than that of ordinary concrete. In sulfate attack environment, the peak stresses of ordinary concrete and rubber concrete all show a trend of increasing first and then decreasing.

(2) Rubber can increase the dissipated strain energy of concrete and reduce the release rate of elastic strain energy of concrete, that is, increase the total strain energy of concrete, thereby improving the ductile deformation and toughness of concrete. It can delay the deterioration of concrete by sulfate, inhibit the penetration and expansion speed of cracks, and improve the sulfate resistance of concrete.

(3) The addition of rubber into concrete significantly reduces the concentration of $SO_4^{2-}$ at different depths inside concrete, improves the sulfate attack resistance of concrete, and reduces the invasion of $SO_4^{2-}$. Due to the workability of rubber particles, the particle gradation of aggregate is optimized and the structure is relatively dense.

(4) The microscopic analysis of concrete samples after sulfate attack is carried out. At the initial stage of corrosion, the surface and internal pores of the concrete provide conditions and channels for sulfate attack. As the corrosion progresses, ettringite and gypsum are generated to fill the internal pores. After further corrosion, a large amount of ettringite produces structural damage and a large number of cracks and holes are generated.

## Data Availability

The data used to support the findings of this study are included within the article.

## Conflicts of Interest

The author declares that there are no conflicts of interest regarding the publication of this paper.

## Acknowledgments

This study was financially supported by Major Natural Science Research Projects of Universities in Anhui Province (KJ2016SD08) and Natural Science Research Projects of Universities in Anhui Province (KJ2019A0917).

## References

[1] K. Chen, D. Wu, L. Xia, Q. Cai, and Z. Zhang, "Geopolymer concrete durability subjected to aggressive environments-a review of influence factors and comparison with ordinary Portland cement," *Construction and Building Materials*, vol. 279, Article ID 122496, 2021.

[2] H. A. Gamal, M. S. El-Feky, Y. R. Alharbi, A. A. Abadel, and M. Kohail, "Enhancement of the concrete durability with hybrid nano materials," *Sustainability*, vol. 13, no. 3, p. 1373, 2021.

[3] H. Cheng, T. Liu, D. Zou, and A. Zhou, "Compressive strength assessment of sulfate-attacked concrete by using

sulfate ions distributions," *Construction and Building Materials*, vol. 293, Article ID 123550, 2021.

[4] J. Stroh, M.-C. Schlegel, E. F. Irassar, B. Meng, and F. Emmerling, "Applying high resolution SyXRD analysis on sulfate attacked concrete field samples," *Cement and Concrete Research*, vol. 66, pp. 19–26, 2014.

[5] J. Wang, D. Niu, H. He, and B. Wang, "Durability degradation of lining shotcrete exposed to compound salt," *China Civil Engineering Journal*, vol. 52, pp. 79–90, 2019.

[6] Q. Wu, Q. Ma, and X. Huang, "Mechanical properties and damage evolution of concrete materials considering sulfate attack," *Materials*, vol. 14, no. 9, p. 2343, 2021.

[7] K. Wang, J. Guo, X. Liu, L. Yang, and P. Zhang, "Effect of dry-wet ratio on pore-structure characteristics of fly ash concrete under sulfate attack," *Materials and Structures*, vol. 54, no. 3, p. 100, 2021.

[8] Z. Jin, W. Sun, Y. Zhang, and J. Jiang, "Damage of concrete in sulfate and chloride solution," *Journal of the Chinese Ceramic Society*, vol. 34, pp. 630–635, 2006.

[9] Y. Zhao, S. Ren, L. Wang et al., "Acoustic emission and physicomechanical properties of concrete under sulfate attack," *Journal of Materials in Civil Engineering*, vol. 33, no. 4, Article ID 04021016, 2021.

[10] R. Sharma and R. A. Khan, "Sulfate resistance of self compacting concrete incorporating copper slag as fine aggregates with mineral admixtures," *Construction and Building Materials*, vol. 287, Article ID 122985, 2021.

[11] Z. Wang, Y. Li, J. Lu, J. Tian, and K. Zhao, "Acoustic emission and physicomechanical properties of concrete under sulfate attack," *Journal of Materials in Civil Engineering*, vol. 111, pp. 56–62, 2020.

[12] X. Lv, Y. Dong, R. Wang, C. Lu, and X. Wang, "Resistance improvement of cement mortar containing silica fume to external sulfate attacks at normal temperature," *Construction and Building Materials*, vol. 258, Article ID 119630, 2020.

[13] V. Vishwakarma, S. Uthaman, R. Dasnamoorthy, and V. Kanagasabai, "Investigation on surface sulfate attack of nanoparticle-modified fly ash concrete," *Environmental Science and Pollution Research*, vol. 27, no. 33, pp. 41372–41380, 2020.

[14] J. Shao, H. Zhu, G. Xue, Y. Yu, S. Mirgan Borito, and W. Jiang, "Mechanical and restrained shrinkage behaviors of cement mortar incorporating waste tire rubber particles and expansive agent," *Construction and Building Materials*, vol. 296, Article ID 123742, 2021.

[15] S. M. A. Qaidi, Y. Z. Dinkha, J. H. Haido, M. H. Ali, and B. A. Tayeh, "Engineering properties of sustainable green concrete incorporating eco-friendly aggregate of crumb rubber: a review," *Journal of Cleaner Production*, vol. 324, Article ID 129251, 2021.

[16] B. S. Thomas, S. Kumar, P. Mehra, R. C. Gupta, M. Joseph, and L. J. Csetenyi, "Abrasion resistance of sustainable green concrete containing waste tire rubber particles," *Construction and Building Materials*, vol. 124, pp. 906–909, 2016.

[17] W. S. Alaloul, M. A. Musarat, B. A Tayeh et al., "Mechanical and deformation properties of rubberized engineered cementitious composite (ECC)," *Case Studies in Construction Materials*, vol. 13, Article ID e00385, 2020.

[18] J. Zhang, G. Zhang, X. Sun et al., "An experimental study on the compressive dynamic performance of rubber concrete under freeze-thaw cycles," *Advances in Civil Engineering*, vol. 2021, pp. 1–12, Article ID 6655799, 2021.

[19] K. Strukar, T. Kalman Šipoš, T. Dokšanović, and H. Rodrigues, "Experimental study of rubberized concrete stress-strain behavior for improving constitutive models," *Materials*, vol. 11, no. 11, p. 2245, 2018.

[20] K. E. Ridgley, A. A. Abouhussien, A. A. Hassan, and B. Colbourne, "Evaluation of abrasion resistance of self-consolidating rubberized concrete by acoustic emission analysis," *Journal of Materials in Civil Engineering*, vol. 30, Article ID 040181196, 2018.

[21] Y. Zhang, Z. Zhao, S. Chen, and W. Sun, "Impact of rubber powder on forst resistance of concrete in water and NaCl solution," *Journal of Southeast University (Natural Science Edition)*, vol. 36, pp. 248–252, 2006.

[22] E. A. H. Alwesabi, B. H. A. Bakar, I. M. H. Alshaikh, A. M. Zeyad, A. Altheeb, and H. Alghamdi, "Experimental investigation on fracture characteristics of plain and rubberized concrete containing hybrid steel-polypropylene fiber," *Structures*, vol. 33, pp. 4421–4432, 2021.

[23] G. Xue, L. Sun, S. Xu, and W. Hou, "Study on compressive properties and meso failure mechanism of rubber concrete," *Journal of Shenyang Jianzhu University(Natural Science)*, vol. 36, pp. 1082–1090, 2020.

[24] S. He and H. Wang, "Orthogonal experimental studies on mix design of high performance concrete," *Industrial Construction*, vol. 8, pp. 8–10+41, 2003.

[25] B. A. Tayeh, O. Ibrahim, and O. Mohamed, "Combined effect of lightweight fine aggregate and micro rubber ash on the properties of cement mortar," *Advances in concrete construction*, vol. 10, no. 6, pp. 537–546, 2020.

[26] Y. Zhou, H. Tian, H. Cui, F. Xing, and L. Sui, "Model for sulfate diffusion depth in concrete under complex aggressive environments and its experimental verification," *Advances in Materials Science and Engineering*, vol. 2015, pp. 1–11, 2015.